ANALOGUE STUDY OF ELECTRON TRAJECTORIES*

By BENJAMIN F. LOGAN, GEORGE R. WELTI AND GEORGE C. SPONSLER
Massachusetts Institute of Technology, Cambridge, Mass.

INTRODUCTION. The advantages of employing analogue computers in the study of dynamic systems are well known. Recently, the Dynamic Analysis and Control Laboratory (D.A.C.L.) at M. I. T. demonstrated another usefulness of simulation techniques by applying the D.A.C.L. Generalized Computer to a problem in electron optics.

In the past, the problem of determining electron trajectories in electrostatic fields specified by boundary potentials usually has been solved by means of rubber-sheet models or by numerical analysis employing potential plots obtained with the aid of electrolytic tanks or resistor-network analogues.[1] A number of investigators have developed automatic electron-trajectory tracers employing various types of electromechanical analyzers in conjunction with electrolytic tanks.[2-8] The most successful of these automatic devices have been those in which some form of differential analyzer was used to integrate directly the equations of motion of the electrons.[4,7] These differential analyzers have been of the rotating-shaft type[9] and, consequently, have traced trajectories rather slowly (e.g., 0.4 in./min.).

In a recent study, standard D.A.C.L. analogue computing components were employed, together with an electrolytic tank, to generate electron trajectories directly at speeds of the order of 1 in./sec. With minor setup changes, the same equipment was used to map the electrostatic field in the tank.

FUNDAMENTAL EQUATIONS

Trajectory Equations. When relativity is neglected, the basic equations of motion for an electron in an electrostatic field are

$$\frac{d^2x}{dt^2} = \frac{e}{m} E_x\,(x,y,z,t) \tag{1}$$

$$\frac{d^2y}{dt^2} = \frac{e}{m} E_y\,(x,y,z,t) \tag{2}$$

$$\frac{d^2z}{dt^2} = \frac{e}{m} E_z\,(x,y,z,t) \tag{3}$$

where E_x, E_y, and E_z are the components of the electric field and e/m is

*Presented at the meeting of the Association, June 23-25, 1954. The research in this paper was supported in part by the Army, Navy, and Air Force under contract with the Massachusetts Institute of Technology.

the charge-to-mass ratio for an electron. Only the cases will be considered in which the equipotential surfaces are parallel cylinders or surfaces of revolution. A coordinate system will be chosen such that

$$z(0) = 0. \tag{4}$$

In the case of cylindrical equipotential surfaces, the z axis will be chosen parallel to the elements of the cylinders in order that

$$E_z(x, y, z, t) = 0. \tag{5}$$

Therefore,

$$\frac{dz}{dt} = \text{constant} = \left.\frac{dz}{dt}\right|_{t=0} \tag{6}$$

Thus, motion in the z direction is independent of the electric field, and the problem reduces to solving equations (1) and (2).

In the case in which the equipotential surfaces are surfaces of revolution, the x axis will be chosen to coincide with the axis of revolution so that

$$E_z \Big|_{z=0} = 0 \tag{7}$$

If it is assumed that

$$\left.\frac{dz}{dt}\right|_{t=0} = 0. \tag{8}$$

then

$$z(t) = 0, \tag{9}$$

and the problem reduces to solving equations (1) and (2) in a more restricted form, that is:

$$\frac{d^2x}{dt^2} = \frac{e}{m} E_x \Big|_{z=0} \tag{10}$$

$$\frac{d^2y}{dt^2} = \frac{e}{m} E_y \Big|_{z=0} \tag{11}$$

Equations (10) and (11) also may be applied to the case of cylindrical equipotential surfaces, since in that case the partial derivatives are independent of z. These equations may be represented by the block diagram of FIGURE 1. A practical computer setup for solving these equations is presented in Section 3.

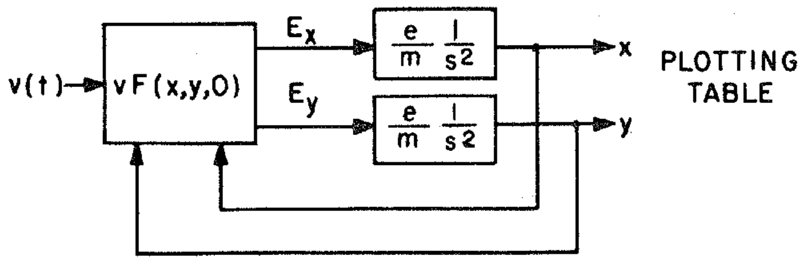

FIGURE 1. Block diagram for trajectory tracing.

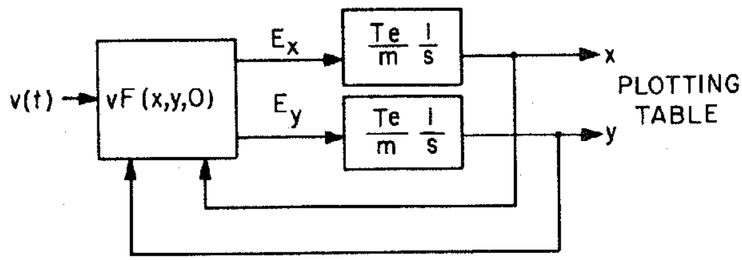

FIGURE 2. Block diagram for flux-line tracing.

Equations for Field Plotting. A means for tracing flux lines in fields of the type discussed in the preceding section is illustrated by the block diagram of FIGURE 2. The corresponding equations are:

$$\frac{dx}{dt} = \frac{Te}{m} E_x \tag{12}$$

$$\frac{dy}{dt} = \frac{Te}{m} E_y \tag{13}$$

where T, an arbitrary constant having the dimensions of time, is introduced to make the equations dimensionally correct. Since the velocity of the tracer is always in the direction of the field, the tracer must describe a field line.

Equipotential lines may be traced in a similar manner, according to the scheme shown in FIGURE 3.

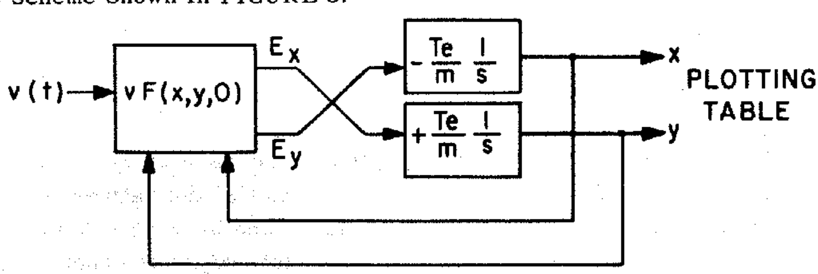

FIGURE 3. Block diagram for tracing equipotential lines.

The corresponding equations are:

$$\frac{dx}{dt} = -\frac{Te}{m} E_y \tag{14}$$

$$\frac{dy}{dt} = +\frac{Te}{m} E_x . \tag{15}$$

Here the resultant velocity of the tracer is always normal to the field; hence, the tracer must describe the intersection of an equipotential surface with the x,y plane.

SIMULATOR SETUP. A simplified simulator setup for trajectory tracing appears in FIGURE 4. The block marked *Function Generator* includes

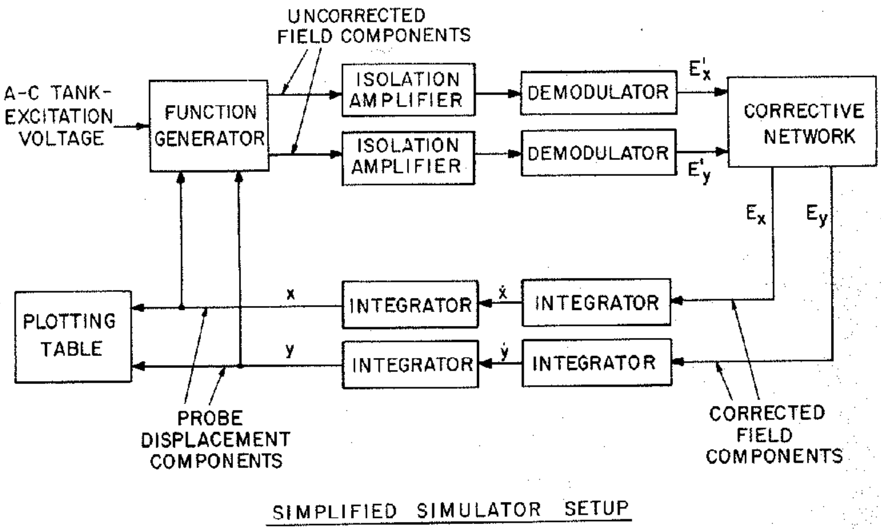

FIGURE 4. **Simplified simulator setup.**

two servomechanisms, the electrolytic tank, and a special probe for measuring two components of the electric field in the tank. The *Isolation Amplifiers* were developed especially for this application and are described later. The remaining blocks in the diagram represent standard Dynamic Analysis and Control Laboratory computing components or networks of such components.

Function Generator. One of the D.A.C.L. function generators[10] was adapted to generate the electric field as a function of x and y. In conventional operation of the function generator a potentiometer mounted on a servo-driven reading head is displaced by a three-dimensional cam having a surface which represents the desired function of the independent variables x and y. For this study, an electrolytic tank was substituted for the cam, and the cam follower and potentiometer were replaced by a probe which measured directly the components of the electric field in the tank.

Electrolytic Tank. The use of the electrolytic tank for plotting electrostatic potential distribution is well known,[1,11] and thorough studies of its capabilities and failings in this application have been made.[1,12] Therefore, little additional information need be given here other than a description of the particular equipment used in this study. The tank was constructed of plexiglass, and the electrolyte chosen was ordinary tap water. The various electrodes immersed in the tank were fabricated of gold-plated brass and gold-sputtered formed pyrex glass. Gold was employed to minimize the polarization difficulties encountered with electrolytic tanks.[12] Also to combat the polarization effects, an a-c voltage (416.7 cps.) was used to excite the tank.

Probe. The probe consisted of three wires of 10-mil diameter spaced approximately 25 mils apart in a "rexolyte" plastic rod, as shown in

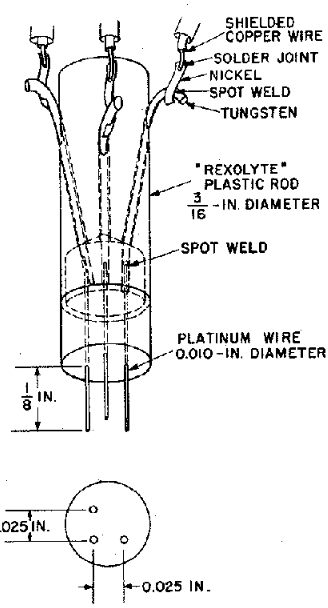

FIGURE 5. Construction details of probe.

FIGURE 5. Platinum wire was employed in the probe to reduce further the effects of electrolyte polarization.[12] The potential difference between two probe wires was assumed to be proportional to the component of the electric field in the plane of the wires.

Measurement Errors. The finite spacing of the probe wires introduces a small error into the measurement of the field components; however, it can be demonstrated easily that this error is negligible if the spacing is small compared to the distance between the probe and the nearest tank electrode or if it is small compared to the spacing between tank electrodes.

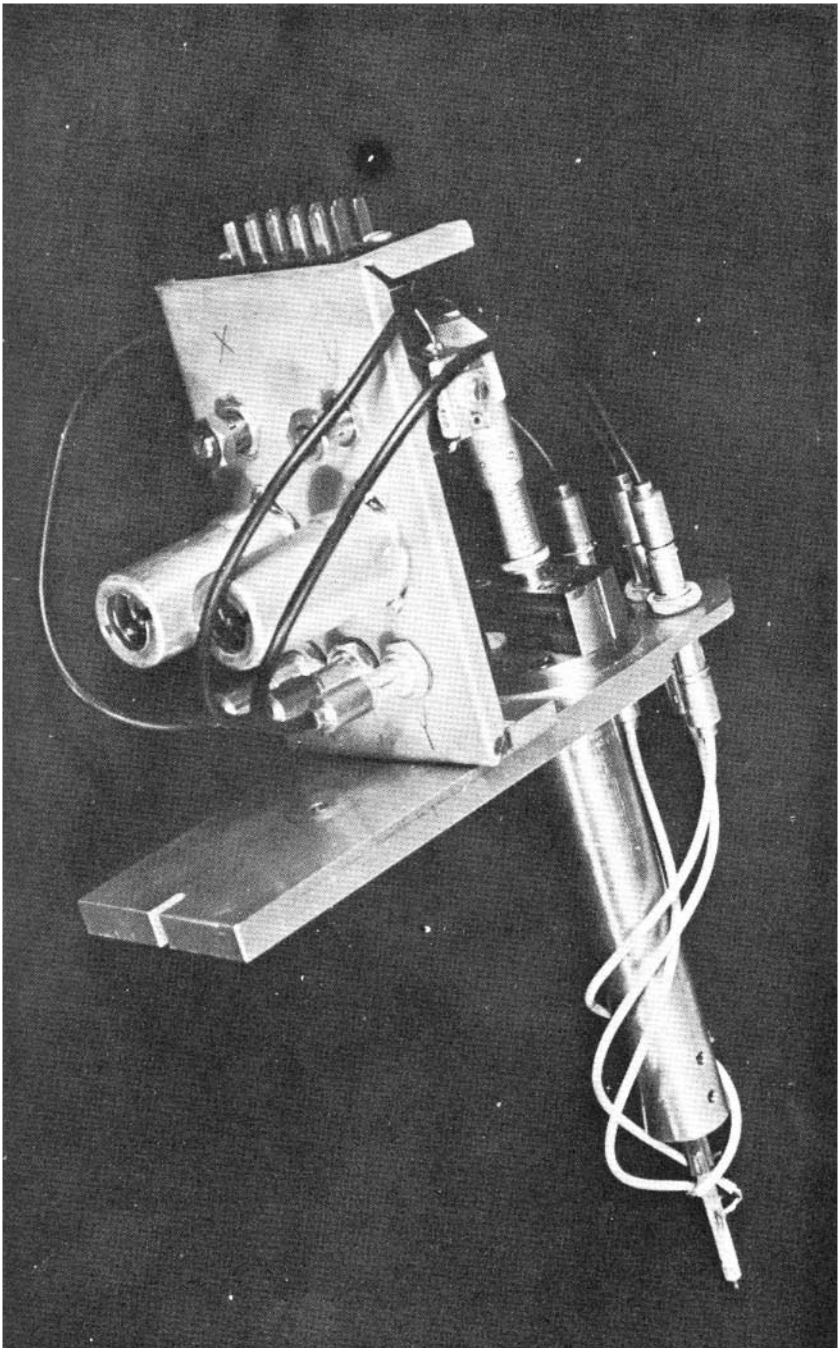

FIGURE 6. Probe assembly.

A serious source of measurement error was the evaporation of the water the level of which was found to drop at the rate of 0.5 mil/min. under average conditions. Originally, it had been planned to immerse the probe wires just barely beneath the surface (e.g., 3 mils); and for this purpose, the probe had been mounted on a micrometer head to permit accurate depth setting (see FIGURE 6). However, evaporation of the water caused such stretching of the meniscus that after a brief time the field measurements in the electrolytic tank were altered greatly. This difficulty was partially remedied by immersing the probe to a depth of 100 mils and then raising it 50 mils, whereupon it could be left for periods greater than one half hour without further adjustment. FIGURE 7 is a typical graph showing the

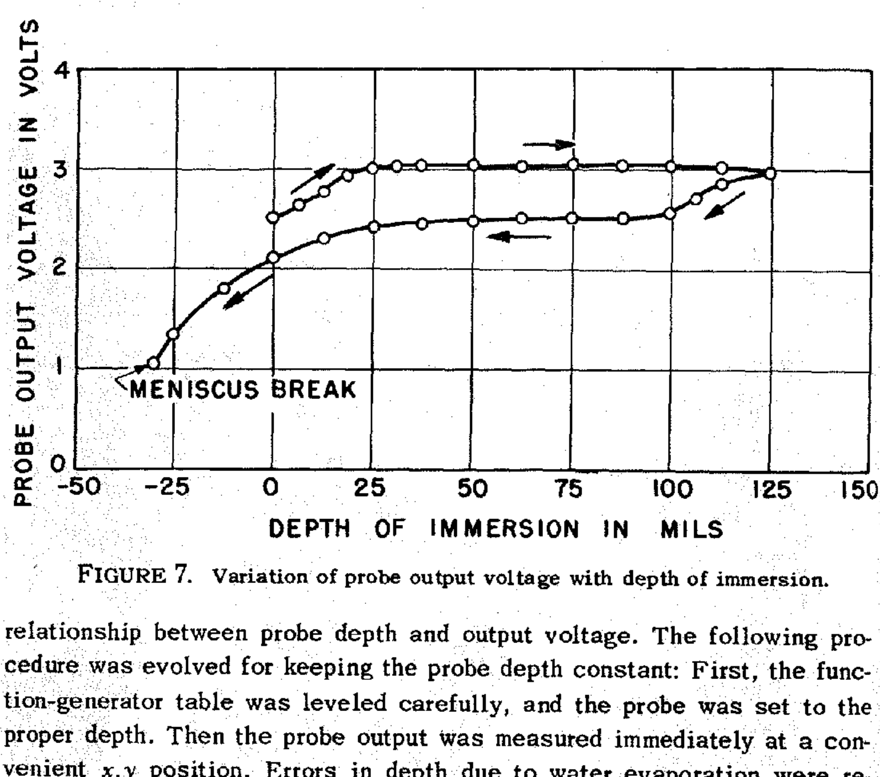

FIGURE 7. Variation of probe output voltage with depth of immersion.

relationship between probe depth and output voltage. The following procedure was evolved for keeping the probe depth constant: First, the function-generator table was leveled carefully, and the probe was set to the proper depth. Then the probe output was measured immediately at a convenient x,y position. Errors in depth due to water evaporation were removed from time to time by returning the probe to the same x,y position and lowering it until the output voltage was restored to its original value.

Before correction, the largest measurement errors were due to improper placement of the probe wires relative to each other and relative to the x and y axis in the tank. The field components E_x' and E_y' measured by the probe differed from the desired components E_x and E_y in two respects: the directions in which they were taken were not parallel to the x and y axis, and their sensitivities were unequal. These two types of discrepancy were corrected by feeding the measured field components through

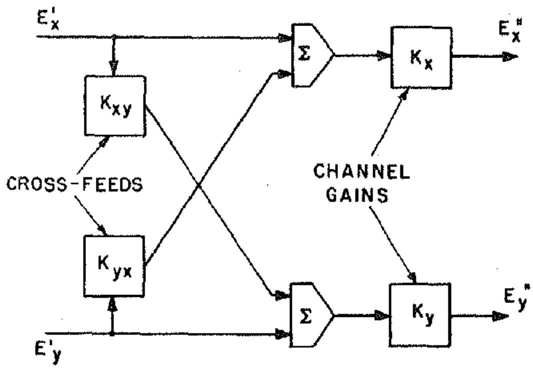

FIGURE 8. Corrective network.

the network shown in FIGURE 8. The outputs E''_x and E''_y of the corrective network can be made equal to E_x and E_y by proper adjustment of the cross-feeds, K_{xy} and K_{yx}, and the channel gains, K_x and K_y. The adjustment procedure is described in Section 4.

Another type of error arises from the perturbation of the electrostatic field caused by the finite diameter of the individual probe wires. This is a difficult problem to analyze exactly. An approximate analysis shows that the effect of finite diameter is analogous to that of improper placement of the probe wires.[14] Then this type of error is also removed by proper adjustment of the corrective network.

Isolation Amplifiers. The output impedance of the probe was high because of the small contact area of the probe electrodes. Consequently,

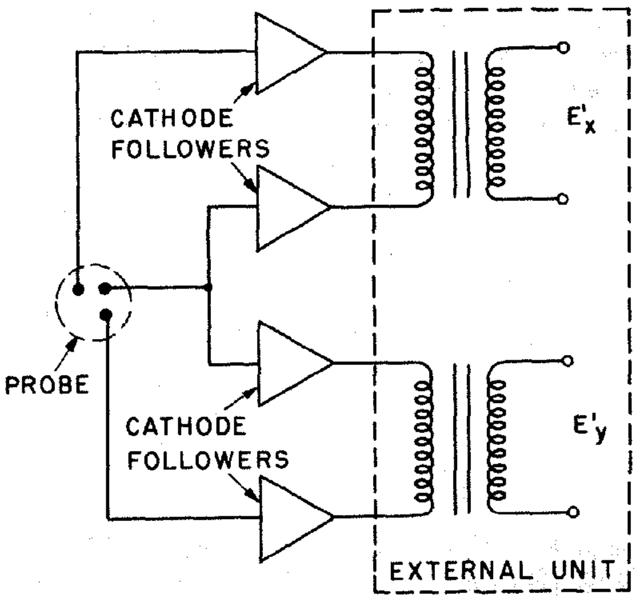

FIGURE 9. Isolation-amplifier unit.

isolation amplifiers having high input impedances were used to prevent loading of the probe in order to keep probe leads short, a compact unit consisting of two simple difference amplifiers was designed for direct mounting on the probe assembly, as shown in FIGURE 6. A simplified diagram of the amplifier unit is shown in FIGURE 9. The voltage sensed by each pair of probe elements was fed to a pair of matched cathode followers. Each pair of cathode followers was provided with balance adjustments. The output of each pair of cathode followers was fed to a difference transformer to yield a voltage proportional to a component of the potential gradient in the electrolytic tank. The outputs of the isolation amplifiers were subject to a zero drift caused by slight gain variations in the cathode followers. As a result, the cathode followers needed to be rebalanced frequently. Balancing was accomplished by trimming the cathode impedances until the outputs of both channels were zero when all tank electrodes were held at the same potential.

CALIBRATION PROCEDURE. In order to calibrate the system, it was necessary to have precise knowledge of the field in the electrolytic tank. With this knowledge, the corrective network could be adjusted, and the proper proportionality between scale factors could be established. Since the magnitude and direction of the field in the "working" tank was unknown, a special tank formed by two concentric circular cylindrical electrodes was constructed for calibration purposes. The electric field at any radius in the calibration tank is a radial vector inversely proportional to the radius.

Adjustment of Corrective Network. Sinusoidal command signals 90° out of phase with each other were fed into the function generator, causing the probe to trace a concentric circular path of radius r in the cylindrical tank. This situation is described by the following equations:

$$x = r \sin \omega t \tag{16}$$

$$y = r \cos \omega t \tag{17}$$

$$E_x = \frac{K}{r} \sin \omega t = \frac{K}{r^2} x \tag{18}$$

$$E_y = \frac{K}{r} \cos \omega t = \frac{K}{r^2} y. \tag{19}$$

With the probe circling in the tank, a Lissajous pattern of E_x'' versus x was plotted automatically, and the cross-feed coefficient K_{yx} (see FIGURE 8) was adjusted until the pattern reduced to a straight line.

Similarly, K_{xy} was adjusted while E''_y versus y was plotted, with the result that

$$E''_x = Ax \tag{20}$$

$$E''_y = By \tag{21}$$

The next step was to plot E''_y versus E''_x and to adjust K_x and K_y until the Lissajous pattern was made to be an exact circle. This adjustment was facilitated by interchanging the inputs to the plotting table and noting the discrepancy between the superimposed plots.

Partial System Checkout. A partial checkout of the system was obtained by using the setup shown in FIGURE 3 to trace equipotential lines in the cylindrical tank. In addition to ensuring the proper operation of two of the four integrators, this procedure provided a sensitive check of the adjustment of the corrective network. If the cross-feeds were adjusted improperly, a spiral, (or in a special case a tilted ellipse) was plotted; if the channel gains were adjusted improperly, a right ellipse was obtained. If a perfect circle were obtained, the partial system was assumed to be operating satisfactorily.

Final Calibration of Complete System. The final step in the calibration procedure was to use the setup of FIGURE 4 with the cylindrical tank to generate electron trajectories. With suitable initial conditions, a circular trajectory can be obtained in the field existing in this tank. The relation between electron velocity and electrode potential difference for this trajectory is calculated readily by equating the centrifugal force of the electron and the centripetal force exerted by the field:

$$\frac{mv_o^2}{r} = e\,E_r \frac{eV_o}{\log \dfrac{r_2}{r_1}} \tag{22}$$

$$v_o^2 = \frac{e}{m} \; \frac{V_o}{\log \dfrac{r_2}{r_1}} \tag{23}$$

where v_o is the velocity of the electron, e/m is the charge-to-mass ratio of the electron, r_2 is the radius of the outer cylinder, r_1 is the radius of the inner cylinder, and V_o is the potential difference between the cylinders. The relation between initial velocity and voltage for a circular trajectory is independent of the trajectory radius r.

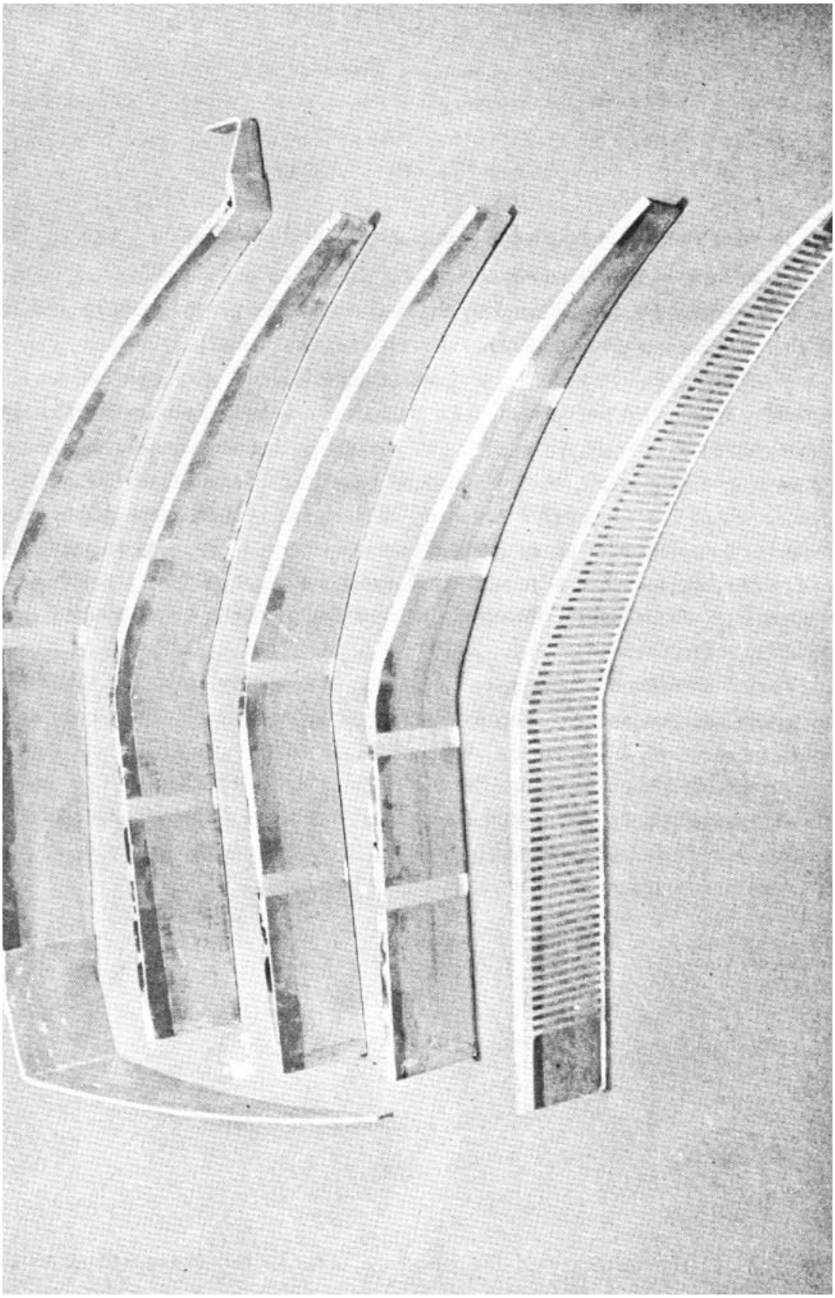

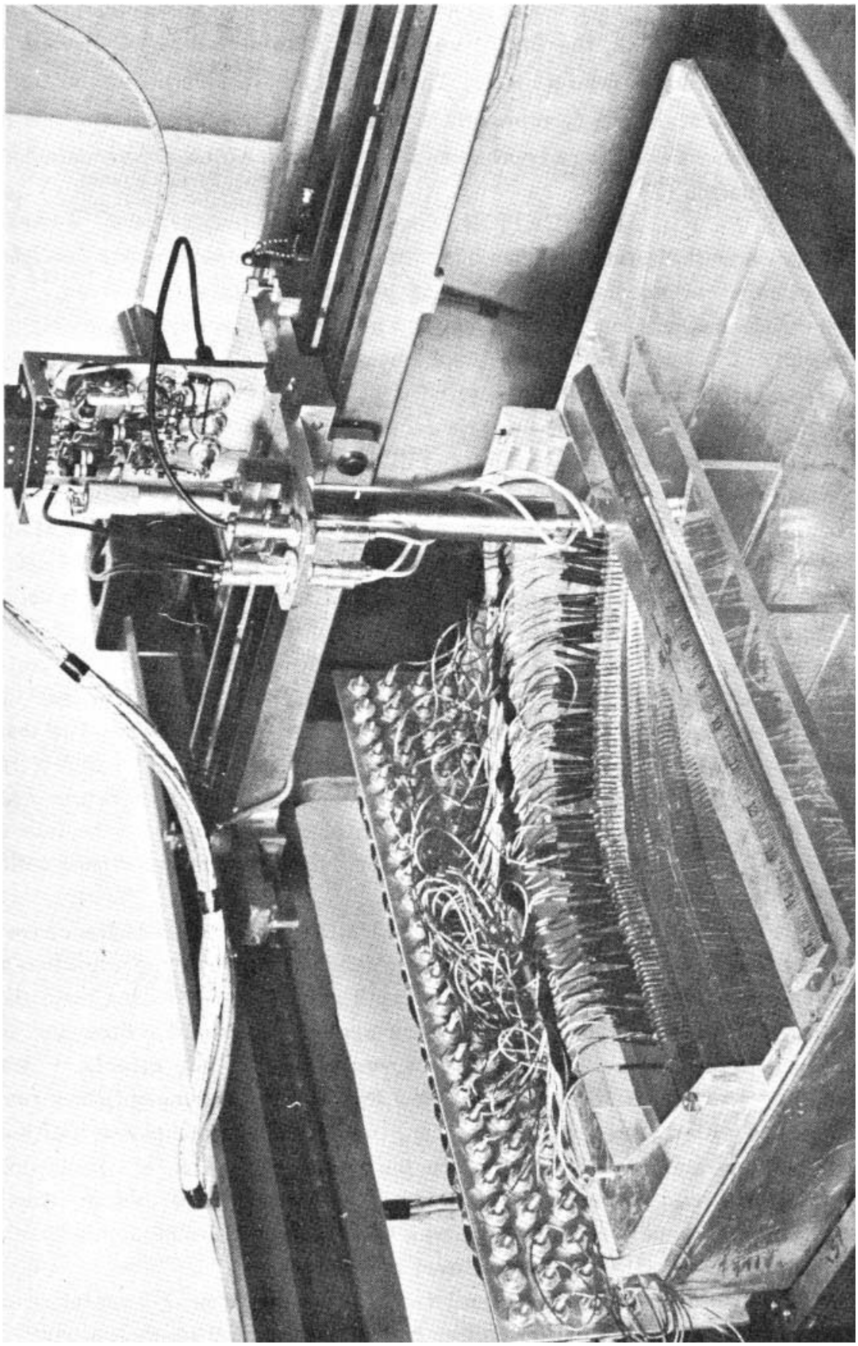

FIGURE 11. Function Generator assembly.

In the calibration procedure, the probe initially was positioned in the cylindrical tank at $x_o = 0$ and $y_o = r$ where $r_1 < r < r_2$. With a given potential across the tank, the initial velocity $\dot{x}_o$ was varied ($\dot{y}_o = 0$) until the resulting trajectory was a circle. The velocity $\dot{x}_o$ to give a circular trajectory then was chosen to represent a desired electron velocity v_o and the actual electrode voltage represented by the tank voltage was calculated from Equation (23).

A SPECIFIC APPLICATION. The electron-trajectory tracer was used to determine the relative merits of several acceleration-electrode configurations in a cathode ray tube utilizing post-deflection acceleration.[13] The electrode assemblies shown in FIGURE 10 were placed in a sloping-bottom tank to simulate a wedge-shaped section of the tube.[14] After the system was calibrated using the cylindrical tank, the tube model was placed in the function generator, and the accelerating electrodes were connected to a multitap low-impedance voltage divider, as shown in FIGURE 11. The probe was positioned initially in the neck of the tube and given an initial velocity representing an electron energy of 2700 electron-volts. Initial deflection angles of 5.5°, 13.5°, 21.5°, and 30° were established by setting in the proper x and y components of the initial velocity. For each deflection angle, trajectories were plotted for maximum accelerating potentials representing 2.7, 5, 7.5, 10, 12.5 and 15 kilovolts. A total of 250 trajectories were traced for six different electrode configurations in less than two days of running time. Some of these were check solutions. The reproducibility of the trajectories was better than ½ per cent. The trajectories showed that a spiral acceleration electrode (*e.g.*, the acceleration potential is applied across a spiral resistance element painted on the tube envelope) resulted in maximum linearity of deflection and maximum deflection sensitivity.

RECOMMENDATIONS AND CONCLUSIONS. Operation of the computer would be simplified and made more reliable by eliminating isolation-amplifier drift and the effects of probe-depth variation. Replacing the cathode followers with high-negative-feedback amplifiers should reduce the drift to negligible values. However, an investigation of the effects of probe loading on field distortion might show that the isolation amplifiers can be replaced with difference transformers, tuned to eliminate phase shifts and to present maximum impedance to the probe. Effects of probe-depth variation could perhaps be eliminated by a new probe design. Another possible approach would be to maintain constant probe depth by automatically controlling the water level in the tank.

The usefulness of an electrolytic tank as a means of generating certain functions of two variables has been demonstrated in an analogue computer study of electron trajectories. Techniques have been developed for calibrating and operating a computer employing electrolytic tanks. These techniques are not restricted to electron-optics problems but may be applied in the study of many field and boundary-condition problems.

References

1. Liebmann, G., "Field Plotting and Ray Tracings in Electron Optics," Advances in Electronics, Vol. II. New York, 1950, Academic Press, p. 101.
2. Gabor, D., "Mechanical Tracer for Electron Trajectories," Nature, Vol. 139, February 27, 1937, p. 373.
3. Langmuir, D. B., "Automatic Plotting of Electron Trajectories," Nature, Vol. 139, June 19, 1937, p. 1066.
4. Blewett, J. B., "Tracing of Electron Trajectories Using the Differential Analyzer," Proc. I.R.E., Vol. 36, No. 1, January, 1948, p. 69.
5. Sander, K. F., C. W. Oatley, and J. G. Yates, "Plotting Electron Trajectories," Nature, Vol. 163, March 12, 1949, p. 403.
6. Cassanas, F., and P. Barchewitz, "Un Traceur Automatique de Trajectories d'Electrons," Jour. de Physics at Radium, Vol. 13, Suppl. Nos. 7, 8, 9, July through September, 1952, p. 6.
7. Sander, K. F., C. W. Oatley and, J. G. Yates, "Factors Affecting the Design of an Automatic Electron-Trajectory Tracer," Proc. I.E.E., Vol. 99, Pt. 3, No. 60, July 1952, p. 169.
8. Sander, K. F., and J. G. Yates, "The Accurate Mapping of Electric Fields in an Electrolytic Tank," Proc. I.E.E., Vol. 100, Pt. 2, No. 74, April, 1953, p. 167.
9. Bush, V., and S. H. Caldwell, "A New Type Differential Analyzer," Jour. Franklin Institute, Vol. 240, October, 1945, p. 255.
10. Welti, G. R., "Generator for Functions of Two Variables," paper presented at General Meeting of Assoc. for Computing Machinery, M.I.T., Cambridge, Mass., September 9–11, 1953.
11. Liebman, G., "Electrical Analogues," Brit. Jour. of Applied Phys. Vol. 4, July, 1953, p. 193.
12. Einstein, P. A., "Factors Limiting the Accuracy of the Electrolytic Plotting Tank," Brit Jour. of Applied Phys., Vol. 2, February, 1951, p. 49.
13. Sponsler, C., "Automatic Electron-Trajectory Tracer Study of Post-Deflection Acceleration," paper to be presented at the I.R.E. National Electron Tube Converence, University of Maine, Ørono, Maine, June, 23–25, 1954.
14. Bowman-Manifold, M., and F. H. Nicoll, "Electrolytic Field-Plotting Trough for Circularly Symmetric Systems," Nature, Vol. 142, July 2, 1938, p. 29.